SIMULATION OF OPTICAL AND ELECTRICAL PROPERTIES OF SOLAR CELLS WITH AL_2O_3/SIN_X REAR DIELECTRIC STACKS

S. Bordihn[1,2], J. A. van Delft[2], M. M. Mandoc[2], J. W. Müller[1] and W. M. M. Kessels[2]
[1]Hanwha Q CELLS GmbH, 06766 Bitterfeld-Wolfen, Germany.
[2]Department of Applied Physics, Eindhoven University of Technology,
5600 MB Eindhoven, The Netherlands.

ABSTRACT: The performance of solar cells with a rear Al_2O_3/SiN_x dielectric passivation stack has been investigated by a combination of optical and electrical simulations. The simulations are based on experimentally obtained surface passivation results and optical properties of the considered Al_2O_3/SiN_x stacks with various Al_2O_3 and SiN_x film thicknesses. In the optical simulations the extended net radiation method was applied. The generated optical results served as input for the electrical simulations which were carried out by using PC1D. The optimum optical thickness of the individual layers of the Al_2O_3/SiN_x stacks was found to be 15 – 30 nm for the Al_2O_3 films and 100 – 120 nm for the SiN_x films.
Keywords: Optical modeling, PC1D simulations, Al_2O_3/SiN_x stacks.

1 INTRODCUTION

The concept of rear dielectric passivated *p*-type Si solar cells with local point contacts [1] attracted considerable attention in the recent years since the rear dielectric material can be deposited by low temperature processes and provides a high surface passivation quality and good thermal stability [2]. The potential of rear dielectric passivation has been demonstrated already many years ago by a 25% record efficiency solar cell [3]. However, this solar cell configuration used thermally grown SiO_2 films which are not suitable for industrially manufactured solar cells. Therefore, alternative dielectric materials were investigated and Al_2O_3 films turned out as a proper alternative for *p*-type Si surfaces. Al_2O_3 layers were already discovered by solar cell researchers more than two decades ago [4] but were re-explored by several groups who reported an excellent quality surface passivation of ALD Al_2O_3 films in 2006 [5, 6]. On solar cell level Schmidt et al. showed the potential of Al_2O_3 films by improving the conversion efficiency of *p*-type Si solar cells. [7]. Recently, it was shown that besides the electrical properties also the optical film properties have to be considered to opmimize the use of Al_2O_3 films as dielectric rear side passivation [8].

This work addresses the optimization of the layer thicknesses of Al_2O_3/SiN_x stacks employed as rear side passivation material in *p*-type Si solar cells. The optimal layer thicknesses were investigated by a combination of electrical and optical simulations. The optical simulations used the extended net radiation method and the electrical simulations were performed using PC1D. The optical properties of the solar cell are implemented in PC1D using the specific front external and rear external input files implemented in PC1D. The input files were generated by the optical simulations. Two spectra are generated: the front external spectrum is the sum of all light that enters the silicon from the front side and the light that is reflected at the front side. The rear external spectrum is the sum of all light that is reflected internally at the rear side of the solar cell. The surface passivation of the Al_2O_3/SiN_x stacks were investigated experimentally and served also as input for the electrical simulations.

2 SURFACE PASSIVATION EXPERIMENTS

The surface passivation study was carried out using high-quality Fz Si samples with a high bulk lifetime to be most sensitive to the surface passivation performance. The shiny etched *n*- and *p*-type Fz Si substrates have a resistivity of 1-2 Ω·cm and 2-3 Ω·cm, respectively. The samples were cleaned in diluted HF (2%) prior to the dielectric passivation layer deposition. Al_2O_3 and SiN_x films were deposited as dielectric materials on both sample sides. For reference purposes the substrates of one sample received only an Al_2O_3 film deposition. The surface passivation performance was investigated after annealing the samples at 400°C for 10 min in nitrogen atmosphere.

The surface passivation performance is expressed in terms of the maximum effective surface recombination velocity $S_{eff,max}$ which was calculated on basis of the injection dependent, effective minority carrier lifetime $\tau_{eff}(\Delta n)$. The $\tau_{eff}(\Delta n)$-curves were obtained by photoconductance decay measurements in transient mode [9]. The $S_{eff,max}$-values are considered as an upper limit and calculated from the $\tau_{eff}(\Delta n)$-curve at $\Delta n = 10^{14}$ cm^{-3} by: $S_{eff,max} = W/2\cdot(\tau_{eff}^{-1}-\tau_{Auger}^{-1})$ taking into account the wafer thickness W and the Auger lifetime τ_{Auger} according to the parameterization proposed by Richter et al. [10].

3 SURFACE PASSIVATION RESULTS

The surface passivation performance of single-layer Al_2O_3 films and Al_2O_3/SiN_x stacks have been compared on Fz Si material in order to be most sensitive to surface recombination and less to the bulk recombination as Fz material provides a high bulk lifetime. The determined $S_{eff,max}$-values are shown in Fig. 1 as a function of the injection level, i.e. the excess carrier density Δn. At $\Delta n > 5\cdot10^{15}$ cm^{-3}, equal $S_{eff,max}$-values are obtained for single-layer Al_2O_3 films and Al_2O_3/SiN_x stacks on *n*- and *p*-type Si substrates. The difference in $S_{eff,max}$-values for $\Delta n < 5\cdot10^{15}$ cm^{-3} can be related to the different doping levels of the substrates [11-13].

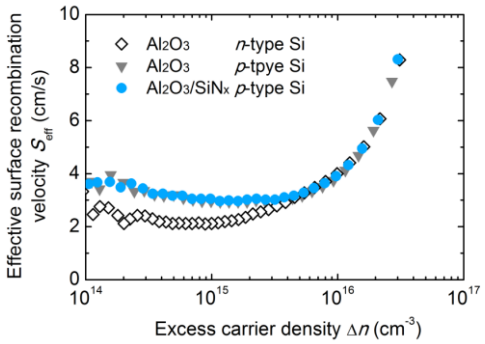

Figure 1: Maximum values of the effective surface recombination velocity $S_{eff,max}$ as a function of the excess carrier density Δn for *n*- and *p*-type Si wafers passivated with single-layer Al_2O_3 films and Al_2O_3/SiN_x stacks.

4 OPTICAL AND ELECTRICAL SIMULATION MODEL

4.1 Optical model

The optimal optical film thicknesses of solar cells with Al_2O_3/SiN_x rear dielectric stacks were investigated by numerical simulations using the extended net radiation method as proposed by Santbergen et al. [14, 15]. This method considered different optical models depending on the type of the interface to take advantage of a reduced computational effort to calculate the propagation of light. Specular reflection is used for smooth interfaces whereas a diffuse reflection is used for rough interfaces [16]. In the case of complex surface structures such as textured surfaces ray tracing simulations were carried out. As a result of the optical simulations two spectra are generated that served as input for the electrical simulations. The first spectrum contains the sum of all light that enters the silicon wafer from the front side or that is reflected at the front side. The second spectrum is the sum of all light that is reflected at the rear side of the solar cell. The layer thicknesses of the Al_2O_3/SiN_x rear dielectric stacks were varied individually, i.e. between 0 and 100 nm for the Al_2O_3 films and between 0 and 120 nm for the SiN_x films. Fig. 2 shows a cross sectional view of the optical model used for the simulations. The front and rear spectra are indicated which are created by the optical simulations and served as input for the electrical simulations. Note that not all possible paths of the light rays are shown for the sake of clarity. A more detailed description of the simulations and the parameters used can be found elsewhere [17].

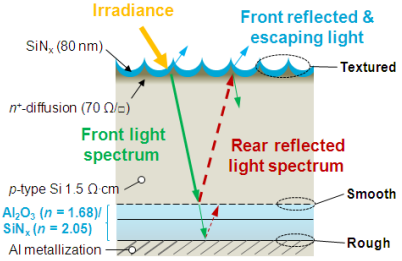

Figure 2: Schematic illustration of the optical simulation model. In the model various types of interfaces are considered. As a result of the optical simulations two spectra are generated, i.e. a front light spectrum and a rear reflected light spectrum which both serves as input files for the electrical simulation using PC1D.

4.2 Electrical model

The electrical simulations were carried out using the numerical device simulation program PC1D [18]. In the electrical simulation model identical device properties were used as in the optical model, i.e. a wafer thickness of 160 µm, the doping profile of the n^+-type emitter layer (resulting in a sheet resistance of 70 Ω/□), the *p*-type base doping density of 10^{16} cm^{-3} (1.5 Ω·cm) as well as the same absorption parameters, i.e. the free carrier absorption [19, 20] and band-to-band absorption model [21]. A front surface recombination velocity of $3 \cdot 10^4$ cm/s [22] was assumed and a bulk lifetime of 260 µs [23]. In the electrical simulations the experimentally determined surface passivation properties of the Al_2O_3/SiN_x rear dielectric stacks were implemented. Hence, a rear surface recombination velocity of 100 cm/s is used as an average value between the experimentally determined passivation performance and the recombination at the metal contacts. These were assumed to cover an area of about 2% and to have a surface recombination velocity of 10^5 cm/s [24].

5 SIMULATION RESULTS

5.1 Validation of optical model

To verify the assumptions made in the optical model the spectral reflection $R(\lambda)$ of a multi-crystalline solar cell with an Al_2O_3/SiN_x rear dielectric passivation stack is measured and compared to the simulation results. The sample is textured on both sides. The wafer front side is coated by an 80 nm SiN_x (n = 2.05) film and the rear side by an Al_2O_3/SiN_x stack which consists of a 20 nm thick Al_2O_3 film and a 100 nm SiN_x layer. The good agreement between the experimental and simulated $R(\lambda)$-data validated the assumptions made in the optical simulations (see Fig. 3).

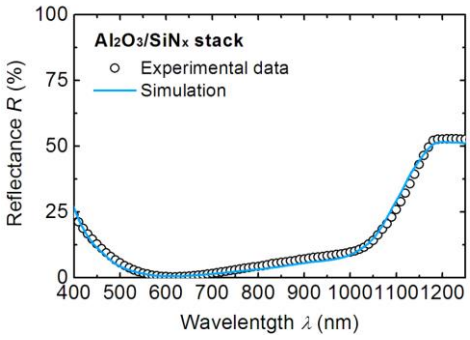

Figure 3: Measured spectral reflectance $R(\lambda)$ of a textured mc-Si wafer with a front side layer of 80 nm SiN_x (n = 2.05) and rear side layer stack of 20 nm Al_2O_3/100 nm SiN_x. The measured $R(\lambda)$-data is compared to results of the optical simulations that used a wafer with an identical layer configuration.

5.2 Simulations of the short circuit current density

The impact of the individually layer thicknesses of the Al_2O_3/SiN_x stacks is expressed in terms of the short circuit current density J_{sc} because this parameter reflects best the changes in the optical properties of a front collecting solar cell. In Fig. 4 the simulated J_{sc}-values are shown for Al_2O_3/SiN_x stacks with different layer thicknesses. For 0 nm SiN_x (i.e. only Al_2O_3 as dielectric)

the J_{sc}-values increases with increasing Al_2O_3 film thickness. However, if the total thickness of the dielectric layer is increased by an additional SiN_x capping layer the differences in J_{sc} can be minimized to a level of minor relevance for the various Al_2O_3 thicknesses. From that it can be concluded that the differences in refractive indices of Al_2O_3 and SiN_x layers plays only a minor role. This is demonstrated in Figure 5 by showing the J_{sc} dependence on the total thickness of the dielectrics for three different Al_2O_3/SiN_x stack systems. In the range between 120 nm and 150 nm the highest J_{sc}-values are obtained for the stacks irrespective of the Al_2O_3 film thickness and therefore, they give the optimum total thickness of the Al_2O_3/SiN_x stacks. It is hypothesized that the slight increase of the J_{sc}-values with increasing Al_2O_3 film thickness is related to interference effects at the rear side of the solar cell.

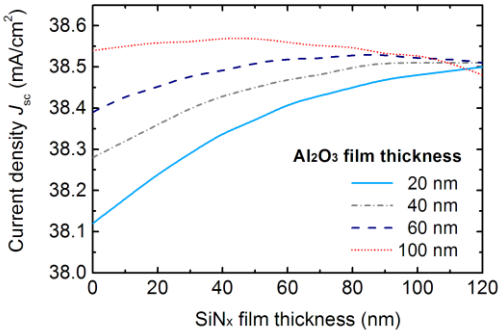

Figure 4: Simulated short-circuit current density J_{sc} as a function of the SiN_x film thicknesses. The different Al_2O_3 film thicknesses are indicated by different line styles and colors.

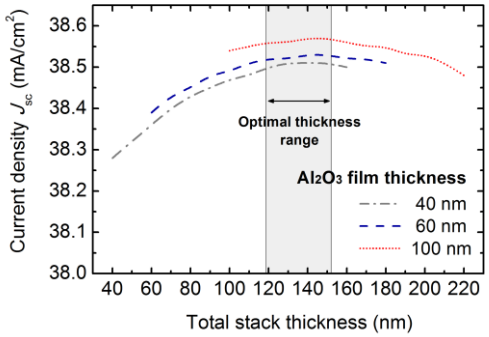

Figure 5: Simulated short-circuit current density J_{sc} as a function of the total thickness of the rear dielectric stack. The different Al_2O_3 film thicknesses are indicated as well as the optimal total thickness range for the Al_2O_3/SiN_x stack.

6 CONCLUSION

In this work a fast and simple simulation approach is presented that combines optical and electrical simulations. For the optical simulation the extended net radiation method was adopted and the simulation results served as input for the electrical simulations carried out with PC1D. A good agreement was found between the optical simulations and experimentally determined spectral reflection results which validate the assumptions made in the optical simulations. It was demonstrated that the optimal total thickness of the rear Al_2O_3/SiN_x stack is between 120 nm and 150 nm. The details of the individual layer thicknesses of Al_2O_3 and SiN_x are only of minor importance as long as the overall layer thickness stated above is met.

7 ACKNOWLEDGEMENTS

This work was supported by the German Federal Ministry for the Environment, Nature Conservation, and Nuclear Safety (BMU) under Contract 0325150 (ALADIN).

8 REFERENCES

[1] R.M. Swanson, Solar Cells 17 (1986) pp. 85−118.
[2] G. Dingemans, W. M. M. Kessels, J. Vac. Sci. Technol. A 30, 4 (2012) pp. 040802-1−040802-27.
[3] J. Zhao, A. Wang, and M.A. Green, Prog. Photovolt: Res. Appl. 7, (1999) pp. 471−474.
[4] R. Hezel and K. Jäger, J. Electrochem. Soc. 136, 2 (1989) pp. 518−523.
[5] G. Agostinelli et al., Sol. Energy Mater. Sol. Cells 90 (2006) pp. 3438−3443.
[6] B. Hoex et al., Appl. Phys. Lett. 89 (2006) pp. 042112-1−042112-3.
[7] J. Schmidt et al., Prog. Photovolt: Res. Appl. 16, 6 (2008) pp. 461−466.
[8] T. Lauermann, B. Fröhlich, G. Hahn, B. Terheiden, in Proc. of 28th IEEE PVSC, Austin, TX, USA (2012) pp. 1710−1715.
[9] R. A. Sinton, A. Cuevas, Appl. Phys. Lett. 69, 17 (1996) pp. 2510−2512.
[10] A. Richter, S. W. Glunz, F. Werner, J. Schmidt, and A. Cuevas, Phys. Rev. B 86 (2012) pp. 165202-1−165202-14.
[11] W.D. Eades and R.M. Swanson, J. Appl. Phys. 58, 11 (1985) pp. 4267−4276.
[12] A.G. Aberle, S.W. Glunz, and W. Warta, J. Appl. Phys. 71, 9 (1992) pp. 4422−4431.
[13] M.J. Kerr, A. Cuevas, Semicond. Sci. Technol. 17 (2002) pp. 166−172.
[14] R. Santbergen and R.J.C. van Zolingen, Sol. Energy Mater. Sol. Cells 92 (2008) pp. 432−444.
[15] R. Santbergen, Ph.D. dissertation, Optical absorption factor of solar cells for PVT systems, Dept. of Mech. Engineering, Eindhoven Univ. of Technology, Eindhoven, The Netherlands 2008.
[16] B.T. Phong, Comm. of the ACM 18, 6 (1975) pp. 311−317.
[17] S. Bordihn, J.A. van Delft, M.M. Mandoc, J.W. Müller and W.M.M. Kessels, IEEE Journal of Photovoltaics 3, 3 (2013) pp. 970−975.
[18] P.A. Basore, D.T. Rover, and A.W. Smith, in Proc. of 20th IEEE PVSC, Las Vegas, NV, USA (1988) pp. 389−396.
[19] P.E. Schmid, Phys. Rev. B 23, 10 (1981) pp. 5331−5336.

[20] M.A. Green, Silicon Solar Cells: Advanced Principles and Practice, Centre for Photovoltaic Devices and Systems, Univ. of New South Wales, Sydney, 1995.
[21] M.A. Green, Sol. Energy Mater. Sol. Cells 92 (2008) pp. 1305−1310.
[22] A. Cuevas, P.A. Basore, G. Giroult-Maltakowski, C. Dubois, J. Appl. Phys. 80, 6 (1996) pp. 3370−3375.
[23] S.W. Glunz, S. Rein, J.Y. Lee, and W. Warta, J. Appl. Phys. 90, 5 (2001) pp. 2397−2404.
[24] B. Fischer, Ph.D. dissertation, Loss analysis of crystalline silicon solar cells using photoconductance and quantum efficiency measurements, Univ. Konstanz, Konstanz, Germany, 2003.